

Development of a diffraction imaging flow cytometer

Kenneth M. Jacobs, Jun Q. Lu, and Xin-Hua Hu*

Department of Physics, East Carolina University, Greenville, North Carolina 27858, USA

*Corresponding author: hux@ecu.edu

Received July 6, 2009; revised August 18, 2009; accepted August 23, 2009;
posted September 3, 2009 (Doc. ID 113909); published September 28, 2009

Diffraction images record angle-resolved distribution of scattered light from a particle excited by coherent light and can correlate highly with the 3D morphology of a particle. We present a jet-in-fluid design of flow chamber for acquisition of clear diffraction images in a laminar flow. Diffraction images of polystyrene spheres of different diameters were acquired and found to correlate highly with the calculated ones based on the Mie theory. Fast Fourier transform analysis indicated that the measured images can be used to extract sphere diameter values. These results demonstrate the significant potentials of high-throughput diffraction imaging flow cytometry for extracting 3D morphological features of cells. © 2009 Optical Society of America
OCIS codes: 110.1650, 120.3890, 120.1530.

Imaging flow cytometry has been pursued in two ways. Noncoherent fluorescence and bright- or dark-field images can be acquired from the flowing particles by using a microscope objective [1,2]. These noncoherent images, however, cannot yield 3D morphological features. Another approach is to acquire a diffraction image of elastically scattered light with a flowing particle illuminated by a highly coherent laser beam [3,4]. A significant problem for this approach is the large background noise, which makes it difficult to extract 3D features. It is thus necessary to eliminate or reduce spurious scattering background caused by the index mismatch at interfaces near the flowing particles. Since these interfaces coexist with a flowing particle in the incident wavefield, typical background subtraction techniques are not applicable. Another issue lies in the demands for accurate and rapid algorithms for pattern analysis of diffraction images of biological cells with complex morphology. Over the past few years, we have conducted studies toward solving both problems by developing accurate numerical tools for modeling of light scattering by biological cells [5–8] and a diffraction imaging method [9]. In this Letter we report a design of flow cytometry that allows the acquisition of clear diffraction images of particles.

Conventional flow cytometer designs employ a cone-shaped nozzle to form a laminar flow in air or a flow channel after exiting the nozzle orifice. Particles carried by the core fluid of small diameter are made to flow in single file before interrogation by light. The interface between the host medium, air or a channeled glass chamber, of the laminar flow and the sheath fluid usually has a large curvature and refractive index difference. Often the medium–sheath index mismatch is much larger than that between the core fluid and a biological cell, which causes strong spurious noise background in a diffraction image. Recently a beam-in-flow design was studied in which a laser beam is coupled and propagated longitudinally into a waveguide also functioning as a microfluidic channel [4]. A CCD camera is attached to an optical window on the waveguide for diffraction imaging.

While this design eliminates the medium–fluid interfaces by directing the incident beam coaxially with the flowing fluid, it has certain limitations for instrumental development. One major disadvantage of the design is the difficulty of maintaining a laminar flow in the waveguide for precise positioning of particles. Another problem lies in the fact that single-particle scattering requires allowing only one particle to flow inside the waveguide. For a waveguide of 2–4 mm in length with flow speeds less than 100 mm/s, this restriction can severely reduce the throughput of the method to 50 particles/s or less. Finally the use of flow channel as waveguides for guiding the incident beam could make it difficult to accommodate multiple incident beams of different wavelengths.

We have studied various designs of flow chambers for eliminating the index mismatch at the medium–sheath interface in a laminar flow. This effort led to a jet-in-fluid design that traces back to an early one for cell counting [10]. Figure 1 presents the schematic for one chamber design that we tested. The core and sheath fluids are pressurized into the coaxially assembled stainless tubing A and B, respectively, from their own syringe-pumped reservoirs. The fluids then enter a square glass cuvette fully filled with water to form a laminar flow jet. The dimension of the cuvette is 10 mm × 10 mm × 75 mm, and a gap space of water is formed between tubing A and B and a fluid exit tubing C 1 mm in diameter. We have investigated different design parameters and found that a core fluid 50 μm in diameter could be obtained near the middle of the gap space if the diameters of A were chosen to be 260 μm (inside) and 510 μm (outside) and B to be 2.4 mm under appropriate differential pressure. Within the laminar flow the particles in the core fluid are forced to flow through the interrogating laser beam in single file when the particle concentration in the core fluid is kept at 10⁴ ml⁻¹ or less. The flowing particles was found to flow quite uniformly in the core fluid within about 25 μm on either side of core fluid center, as shown by the centers of diffraction images in Fig. 2. The size of the gap space along the z axis was set at 4 mm for introducing multiple light

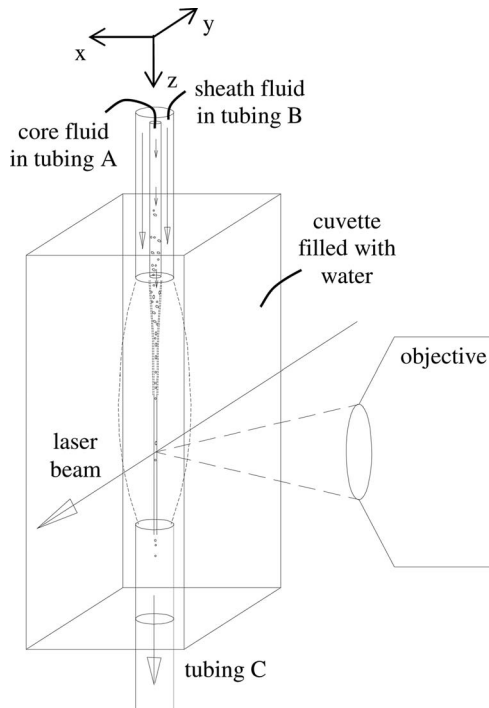


Fig. 1. Schematic of the jet-in-fluid flow chamber (not to scale in the z direction). The short dashed curves indicate the interface between the sheath fluid and cuvette fluid, while the long dashed lines indicate the cone angle of light collection by the microscope objective.

beams along the x and y axes to excite a flowing particle. The scattered light was acquired in an angular region centered along the x axis by a split-view imaging system with a microscope objective, a beam splitter, tube lenses, and two CCD cameras [9]. If all three fluids in core, sheath, and cuvette are water or water based, such as cell culture, no mismatch of real refractive index exists at the medium–sheath interface within the field of view of the CCD cameras. At the focused position (see discussion below) the size of the

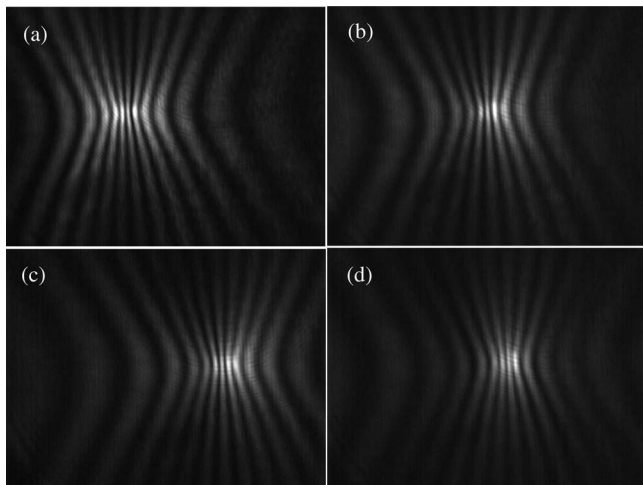


Fig. 2. Measured diffraction images of polystyrene sphere of $9.6 \mu\text{m}$ in nominal diameter with a laser beam of 532 nm in wavelength at different flow speeds of the core fluid: (a) 4.4 mm/s , (b) 6.8 mm/s , (c) 10 mm/s , (d) 14 mm/s . The field of view of these images at the focused position of $x=0$ is $140 \times 180 \mu\text{m}$, and the images were acquired at $x=200 \mu\text{m}$.

field of view along the z axis is $140 \mu\text{m}$, much smaller than the gap space size. Polystyrene spheres of different diameters were used to validate the diffraction imaging flow cytometer with deionized water for all three fluids.

The imaging system was focused first at spheres in the core fluid under a noncoherent illumination to establish a reference position of $x=0$. By varying the CCD camera's exposure time from 1 to 100 ms, the speed of flowing spheres can be determined from the blurred projection of flowing spheres along the z axis during the exposure time or from the fluid flow rate and size of the core fluid. Within the range of differential pressure for maintaining the laminar flow condition, we obtained the flow speed of multiple spheres against their lateral positions in the core fluid. In the gap space and near the lower ends of tubing A and B, the core fluid diameter is about $200 \mu\text{m}$, and the flow speed was found to reach a peak value at the center and decrease parabolically toward the edge of the core, as expected from the Hagen–Poiseuille condition of viscosity flow. The core fluid diameter reduces to $50 \mu\text{m}$ at the center of the gap space, and the flow speed v there can be varied between 2 and 16 mm/s by adjusting the differential pressure between the core and sheath. When $v \sim 10 \text{ mm/s}$, the Reynolds number of the core fluid can be calculated to be about 1, indicating a viscous-loss-dominated laminar flow regime as expected.

By replacing the noncoherent illumination with a laser beam, we then acquired diffraction images of flowing spheres by translating the imaging system to a defocused position of $x=200 \mu\text{m}$ toward the flow chamber [9]. A cw diode-pumped solid-state laser was used to produce the incident beam at 532 nm with a linear polarization of 45° from the horizontal direction. The incident beam was collimated, expanded, and focused at the core fluid with a diameter of about $60 \mu\text{m}$ and an incident power at between 10 and 22 mW for different particles. Figure 2 presents diffraction images acquired from polystyrene spheres of $9.6 \mu\text{m}$ in diameter at different flow speeds. At an exposure time of $50 \mu\text{s}$, a sphere moves $0.8 \mu\text{m}$ at a flow speed of 16 mm/s , and the images in Fig. 2 show clearly that flow speed at this value or less causes no blurring. Subsequent diffraction imaging of spheres was performed with the speed set between 2 and 16 mm/s and exposure time fixed at $50 \mu\text{s}$.

Figure 3(a)–3(f) show the diffraction images of polystyrene sphere with different diameters d and projection images of light scatters calculated from the Mie theory. Fast Fourier transform analysis was carried out on the measured images with 1200 pixels along the z axis and 1600 along the y axis and Δ as the pixel-to-pixel distance. The results shown in Fig. 3(g) are the power spectra of these images, with the dc component shifted to $f_y=800(1/\Delta)$ and $f_z=600(1/\Delta)$, along the f_y axis between 650 and $950(1/\Delta)$. The calculated images were obtained from the angle-resolved S_{11} elements of the Mueller matrix [5], assuming the refractive index of the host medium to be $n_h=1.334$ for water and $n_s=1.588$ for polystyrene spheres [11] at the wavelength of 532 nm . The

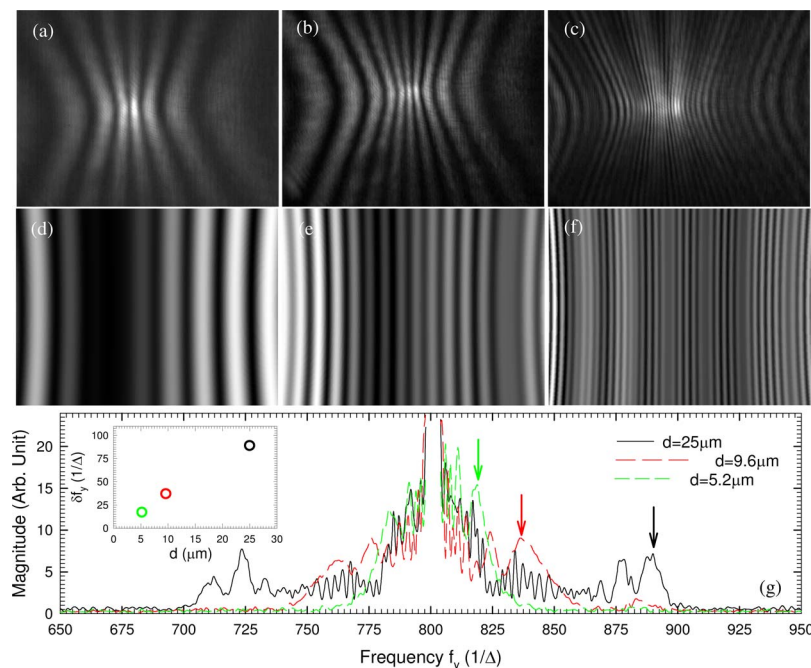


Fig. 3. (Color online) Top and middle panels, measured diffraction images of polystyrene spheres with a laser beam of 532 nm in wavelength and different nominal diameters and flow speeds of (a) 5.2 μm at 13 mm/s, (b) 9.6 μm at 4.4 mm/s, and (c) 25 μm at 14 mm/s and calculated diffraction images based on the Mie theory for single spheres ($n_s = 1.588$) immersed in water ($n_h = 1.334$) with different diameters of (d) 5.2 μm , (e) 9.6 μm , and (f) 25 μm . Bottom panel, (g) fast Fourier transform power spectra of the measured diffraction images at $f_z = 600(1/\Delta)$ with the dc component removed and the arrows indicating selected peaks. Inset, frequency shift of the selected peaks versus nominal sphere diameters.

only adjustable parameter for image calculation is a half-cone angle of projection, which determines the number of fringes in the images, and it was chosen to be 18° based on the comparison for the sphere of $d = 5.2 \mu\text{m}$. We note here that the calculated images were obtained by projection of the scattered light from the sphere on a $y-z$ plane with no consideration of the glass cuvette, objective, and tube lens. Comparison of the measured and calculated images in Fig. 3 reveals a high degree of correlation in the fringe patterns, and the fast Fourier transform results indicated the feasibility of extracting morphological features from the measured data. The main differences lie in the increasing degree of curling of the fringe patterns in the off-center region toward the peripheral and the appearance of a bright center in the measured images, which may be attributed to the simple projection and the use of a plane wave, instead of a Gaussian beam, in the Mie-based calculations. Modeling improvement should account for these differences.

In this report we validated a flow cytometer consisting of a jet-in-fluid chamber design and a split-view imaging system. This design eliminates the medium-sheath index mismatch for high-contrast diffraction imaging, and provides a large gap space to accommodate multiple beams and ease for alignment. We demonstrated that with the current design the particle positioning error is about 25 μm , which can be further reduced with a better nozzle design, smaller gap space, machining improvement, and higher flow speed. With a fast CCD camera of high

sensitivity, high throughput of 1000 cells/s is achievable with the core fluid speed increased to 100 mm/s.

The authors thank Dr. Li V. Yang and Dr. Junhua Ding for stimulating discussions on cell morphology and pattern recognition. This research was supported in part by a National Institutes of Health (NIH) grant (1R15GM70798-01).

References

1. T. Lindmo and H. B. Steen, *Biophys. J.* **28**, 33 (1979).
2. T. C. George, D. A. Basiji, B. E. Hall, D. H. Lynch, W. E. Orty, D. J. Perry, M. J. Seo, C. A. Zimmerman, and P. J. Morrissey, *Cytometry* **59**, 237 (2004).
3. J. Neukammer, C. Gohlke, A. Hope, T. Wessel, and H. Rinneberg, *Appl. Opt.* **42**, 6388 (2003).
4. X. T. Su, K. Singh, C. Capjack, J. Petracek, C. Backhouse, and W. Rozmus, *J. Biomed. Opt.* **13**, 024024 (2008).
5. J. Q. Lu, P. Yang, and X. H. Hu, *J. Biomed. Opt.* **10**, 024022 (2005).
6. R. S. Brock, X. H. Hu, P. Yang, and J. Q. Lu, *Opt. Express* **13**, 5279 (2005).
7. R. S. Brock, X. H. Hu, D. A. Weidner, J. R. Mourant, and J. Q. Lu, *J. Quant. Spectrosc. Radiat. Transf.* **102**, 25 (2006).
8. M. A. Yurkin, A. G. Hoekstra, R. S. Brock, and J. Q. Lu, *Opt. Express* **15**, 17902 (2007).
9. K. M. Jacobs, L. V. Yang, J. Ding, A. E. Ekpenyong, R. Castellone, J. Q. Lu, and X. H. Hu, *J. Biophotonics* **2**, 521 (2009).
10. P. J. Crosland-Taylor, *Nature* **171**, 37 (1953).
11. X. Ma, J. Q. Lu, R. S. Brock, K. M. Jacobs, P. Yang, and X. H. Hu, *Phys. Med. Biol.* **48**, 4165 (2003).